POLITYKA ENERGETYCZNA – ENERGY POLICY JOURNAL

2026 ✦ Volume 29 ✦ Issue 2 ✦ 165–186

DOI: 10.33223/epj/127921

Suzan Abdulrhman Hameed[1], Hussein Hayder Mohammed Ali[2], Shahen Mohammed Fakhraldin[3], Furqan Haider Mohammed Ali[4]

Enhancing the thermal efficiency of solar stills using magnesium oxide nanoparticles in a phase change material on a rotating hollow drum

Abstract: This study experimentally investigates the enhancement of thermal efficiency and freshwater productivity in a double-slope solar still through the integration of a rotating hollow metal cylinder combined with nano-enhanced phase change material (NPCM). Paraffin wax served as the latent heat storage medium, while magnesium oxide (MgO) nanoparticles at 1% volumetric concentration were dispersed to improve thermal conductivity and heat distribution. The nanofluid was prepared via mechanical stirring and ultrasonic dispersion to ensure uniform stability. Field tests were conducted in Kirkuk, Iraq, from February to April 2025 under clear-sky conditions. The modified system achieved a maximum productivity of about 3,400 ml/m^2·day at 0.25 rpm and 3 cm

✉ Corresponding Author: Hussein Hayder Mohammed Ali; e-mail: hussein_kahia@ntu.edu.iq

[1] Kirkuk Technical Engineering College, Northern Technical University; Renewable Energy Research Center Kirkuk, Northern Technical University, Iraq; ORCID iD: 0009-0004-6443-4702; e-mail: suzan.abdulrahman24gs@ntu.edu.iq

[2] Kirkuk Technical Engineering College, Northern Technical University; Renewable Energy Research Center Kirkuk, Northern Technical University, Iraq; ORCID iD: 0000-0003-4264-400X; e-mail: hussein_kahia@ntu.edu.iq

[3] Kirkuk Technical Engineering College, Northern Technical University; Renewable Energy Research Center Kirkuk, Northern Technical University, Iraq; ORCID iD: 0000-0002-7240-5459; e-mail: shahen.fakhraldin@ntu.edu.iq

[4] Kirkuk Technical Engineering College, Northern Technical University; Renewable Energy Research Center Kirkuk, Northern Technical University, Iraq; ORCID iD: 0009-0004-5491-3224; e-mail: furqan.haider.m.ali@ntu.edu.iq

water depth, which is more than six times higher than the 520 ml/m^2·day of the conventional still. Incorporating MgO nanoparticles raised the PCM tube temperature to 62°C compared to 46°C without additives, enhancing evaporation rates and extending production into nighttime hours. The improved design attained a peak thermal efficiency of 90%, outperforming PCM-only (66.5%) and smooth-cylinder (52.5%) systems. These gains are attributed to increased heat transfer surface area, superior thermal conductivity, and optimized rotational control. Compared with previous designs, the copper-tube cylinder with NPCM showed superior performance. Future studies should examine varying nanoparticle types, higher rotation-speed adaptability, and hybrid solar collector integration to further optimize cost-effectiveness and scalability in arid regions.

Keywords: thermal efficiency, magnesium oxide nanoparticles, phase change materials (PCM), solar still, rotating hollow drum

Introduction

Water scarcity is among the most serious global concerns, especially in arid and semi-arid areas where reliable access to potable water is limited. Reports indicate that nearly 25% of the global population lacks access to safely managed drinking water services, and this figure is expected to rise as a result of climate change, population expansion, and inefficient water resource management (Ahmed et al. 2019; Zarda et al. 2022; Qader et al. 2023). Tackling the dual issues of water scarcity and pollution calls for sustainable solutions, where renewable energy resources serve as a key component. Utilizing clean sources such as solar, wind, ocean, and geothermal energy helps decrease dependence on fossil fuels and reduce environmental harm. Among these, solar energy stands out as a viable and increasingly accessible alternative. Thanks to advances in photovoltaic technology, solar energy can now be harnessed even in remote, off-grid locations, contributing significantly to water and energy security (Bayraktar et al. 2022). Solar water distillation utilizes the sun's energy to transform saline water into drinkable distilled water. This study employs two solar still configurations: one conventional and the other enhanced with a rotating hollow metal cylinder. It is designed to maximize solar absorption and improve water yield. The performance of single-effect horizontal solar stills is typically evaluated based on the efficiency of their internal components (Hussein et al. 2024; Qader et al. 2023). However, a primary drawback of this technology is its relatively low output (Chaichan and Kazem 2018; Qader et al. 2024; Yousef and Hassan 2019). To improve productivity, several enhancement strategies have been developed, including the incorporation of phase change materials (PCMs), sponge structures, sand, and other absorptive substances. Among these, PCMs have proven to be particularly efficient in heat storage and release, functioning as both latent and sensible heat storage media. Their non-corrosive nature and high thermal stability make them highly suitable for high-temperature thermal storage systems (Ali and Ahmed 2023, 2024; Ali et al. 2025; Rufuss et al. 2019). Selecting an appropriate PCM depends on several

key parameters such as melting point, density, thermal durability, and suitability for the target application. Materials like paraffin wax (PW), fatty acids, and salt hydrates are commonly used in thermal storage due to their ability to absorb and release significant thermal energy over narrow temperature ranges. Paraffin wax, in particular, has a melting point between 40 and 90°C, making it ideal for a range of solar and electrical heating applications (Nagaraju et al. 2022). Research has shown that integrating PCMs into solar distillation systems can boost their thermal efficiency by up to 40% (Asbik et al. 2016). One study employed a parabolic trough collector in combination with a shell-and-tube heat exchanger to generate steam for desalination, achieving 42% thermal efficiency with PCM versus 30% without (Kateshia and Lakhera 2022). Another experimental setup utilized copper cylinders filled with three different PCMs, paraffin wax, stearic acid, and lauric acid, placed at equal distances within the basin at varying water depths. The use of these PCMs improved distillate productivity by 1,120, 1,050, and 950 ml/$m^2 \cdot$day, respectively (Miri et al. 2023). A paraffin wax-based still achieved a distillate yield of 3.96 kg/m^2, marking a 28.14% increase over conventional stills. Additionally, adding floating wicks to the PCM-enhanced basin further increased yield by 32% (Sonker et al. 2019). Other studies also examined the effect of incorporating nanoparticles into PCM-based solar stills with different absorber geometries. Compared to conventional models, these advanced systems significantly improved productivity by 218% in tubular designs, 149% in single-slope basins, and 125% in pyramidal types, with nighttime yields also increasing by as much as 235% (Dhindsa 2021). Nanotechnology offers a novel approach to enhancing thermal energy storage systems by modifying PCMs at the nanoscale. One effective strategy involves dispersing nanoparticles, such as graphene, carbon nanotubes, or metal oxides, within the PCM matrix to improve its thermal conductivity. Due to their large surface area-to-volume ratio, these nanomaterials facilitate more efficient heat transfer, thereby accelerating thermal response and boosting the overall performance of the storage system (Singh et al. 2023; Kedar et al. 2021; Motahar et al. 2014). The integration of a graphite plate, characterized by its high thermal conductivity, into paraffin wax has led to a significant enhancement in the overall efficiency of the solar still. This modification resulted in a 62% improvement in water production during daylight hours and an impressive 235% increase during nighttime operation (Yadav et al. 2021). Three solar stills of identical geometrical specifications were constructed for comparative analysis: a conventional model, a system incorporating PCM, and another enhanced with a nano-enhanced PCM (NPCM) consisting of paraffin wax mixed with 0.5% by mass of silica nanoparticles. The experimental findings revealed that the use of PCM and NPCM contributed to an increase in freshwater yield by 51.22% and 67.07%, respectively, compared to the conventional unit (Rufuss et al. 2022). Işık and EL 2024 conducted an experimental study to enhance the performance of conventional single-slope basin-type solar stills by incorporating PCMs and graphene-based nanoparticles. Calcium chloride hexahydrate ($CaCl_2 \cdot 6H_2O$) was used as the primary PCM due to its high latent heat storage capacity, while strontium chloride hexahydrate ($SrCl_2 \cdot 6H_2O$) was added as a nucleating agent to mitigate supercooling. Graphene oxide (GO) and graphene nanoplatelets (GNP) were introduced to improve solar absorption through their photothermal properties. The integration of GO with the PCM-nucleating agent combination resulted in the highest water

yield of 5,424 ml/$m^2 \cdot$day and a 54.44% increase in efficiency compared to the conventional still. The system using GNP achieved 5,032 ml/$m^2 \cdot$day, indicating an 8% lower performance than the GO-based configuration. This study encompassed an assessment of the economic viability of both traditional and improved solar stills. The cost for the traditional still is approximately 87 dinars per liter produced, whereas for the improved still it is 65 dinars per liter. Shamshir et al. (2017) conducted a series of experiments under four distinct operating scenarios: (1) introducing 0.5% graphite flake nanoparticles into water, (2) incorporating the nanoparticles into a PCM, (3) combining the nanoparticles with a film cooling system, and (4) integrating all three modifications simultaneously. Among these, the fourth configuration yielded the most favorable outcomes, surpassing the individual performance enhancements observed in scenarios one through three.

Recent advances in solar thermal systems highlight how nanomaterials and innovative designs can significantly enhance energy and water production efficiency. Abu-Hamdeh et al. (2021) numerically investigated molten salt and SiO_2 nanofluids in a solar tower cycle, demonstrating that integrating nanofluids and optimizing the arrangement of preheater heat exchangers increased plant efficiency by up to 3%, particularly under the hot climatic conditions of Jeddah. While their work focused on large-scale power generation, Alizadeh et al. (2021) applied artificial intelligence to predict natural convection heat transfer in oscillating cavities filled with CuO nanofluid, revealing that oscillation amplitude and magnetic fields strongly influence heat transfer. This approach illustrates how AI can reduce computational costs and improve predictive accuracy for complex thermal systems. At the desalination scale, Asadpourian and Ameri (2021) experimentally demonstrated that CuO-GO nanocomposites in basin-type solar stills can boost freshwater yield by up to 91.7%, particularly at 0.3 mass% concentration; however, they also observed that excessive water depth reduces performance, highlighting design-operation trade-offs. Similarly, Manoj Kumar et al. (2021) examined conventional single-slope stills enhanced with phase change and nano-phase change materials, with silica nanoparticle-based PCM increasing productivity by 67%, indicating the value of thermal storage for diurnal operation. Complementary to these studies, Fattahi (2021) numerically compared different cross-section geometries in parabolic solar receivers and found that rectangular ducts yield the best thermal performance, achieving up to 72% higher Nusselt numbers while maintaining lower pressure drop than triangular or trapezoidal channels. Taken together, these investigations suggest that nanomaterials (CuO, GO, SiO_2), hybrid AI-CFD modeling, and geometric optimization are synergistic strategies that can be tailored to either small-scale water desalination or large-scale solar power generation, with future work needed to evaluate long-term stability, cost, and environmental impacts of nanofluid use under real-world conditions. In this study, a comparative analysis is carried out between a conventional solar still and a modified system using various concentrations of NPCM. The objective is to evaluate how different NPCM ratios affect thermal conductivity, heat storage capacity, and overall system performance, ultimately identifying the optimal composite.

2. Experimental methodologies

The proposed solar distillation system is a modified solar still designed to improve freshwater productivity through enhanced thermal management. The structure resembles an insulated chamber and incorporates a central hollow cylinder partially submerged in water. This cylinder is coated with a black opaque material to maximize solar absorption and is capable of continuous rotation. Surrounding the cylinder are eight equally spaced copper pipes filled with NPCM, as shown in Figure 1, composed of paraffin wax and dispersed nanoparticles. These pipes are strategically positioned to increase the total surface area available for thermal interaction and to provide uniform heat distribution within the basin. As the solar radiation intensity varies throughout the day, the rotational speed of the hollow cylinder adjusts accordingly, accelerating with higher irradiance and slowing under reduced conditions. During operation, the rotating cylinder forms a thin film of water on its surface, which evaporates rapidly due to elevated temperatures. This mechanism enhances the evaporation rate and contributes to improved system efficiency. The transparent glass cover has dimensions of 2.08 m in length, 1.22 m in width, and 1 mm in thickness. The hollow cylinder has a diameter of 0.66 m and a length of 1.22 m, with a combined internal and external effective surface area of approximately 5 m^2. The cylinder is mounted on a hollow aluminum shaft supported by universal bearings with a 0.05 mm diameter. Rotation is achieved via a pulley system driven by a DC motor. The motor is connected to a 0.06 m pulley, which in turn drives a 0.24 m pulley attached to the main shaft. A speed control unit is integrated to modulate motor performance in response to changing solar input, ensuring optimal thermal interaction and water evaporation. This system configuration aims to enhance

Fig. 1. A hollow reel with copper tubes fixed on it and painted with opaque black paint

Rys. 1. Pusta szpula z przymocowanymi do niej miedzianymi rurkami, pomalowana nieprzezroczystą czarną farbą

solar energy utilization, improve thermal storage performance, and ultimately increase the yield of distilled water, making it particularly suitable for deployment in arid and resource-limited regions.

2.1. Preparation of PCM with nanoparticles

In the initial stage of nanofluid preparation, a predetermined quantity of paraffin wax granules is carefully measured and placed into a clean, dry flask for storage. This is followed by the accurate weighing of magnesium oxide (MgO) nanoparticles, which serve as the dispersed phase in the nanofluid mixture, as seen in Table 1. To melt the wax, a laboratory-grade hot plate equipped with a temperature control unit is used. The measured wax, typically 150 grams for each experimental tube, is gradually heated until it transitions into a fully liquid state. Once the paraffin wax is completely melted, the preparation of the nanofluid continues by incorporating the nanoparticles. The number of nanoparticles required is calculated to achieve a volumetric concentration of 1%, ensuring consistent formulation across all samples. The selected concentration is based on optimizing the thermal performance while maintaining the stability and dispersion of the nanofluid. Two distinct methods are utilized to mix the MgO nanoparticles into the molten wax, ensuring uniform distribution as shown in Figure 2.

Table 1. Properties of magnesium oxide (MgO) nanoparticles

Tabela 1. Właściwości nanocząstek tlenku magnezu (MgO)

Property	Value
Chemical formula	MgO
Molecular weight	40.30 g/mol
Nano size	10–100 nm
Density	3.58 g/cm^3
Melting point	2,852°C
Thermal conductivity	45–60 W/m.K
Specific heat capacity (Cp)	0.94 J/g.K
Function in solar stills	Thermal conductivity enhancer in PCM

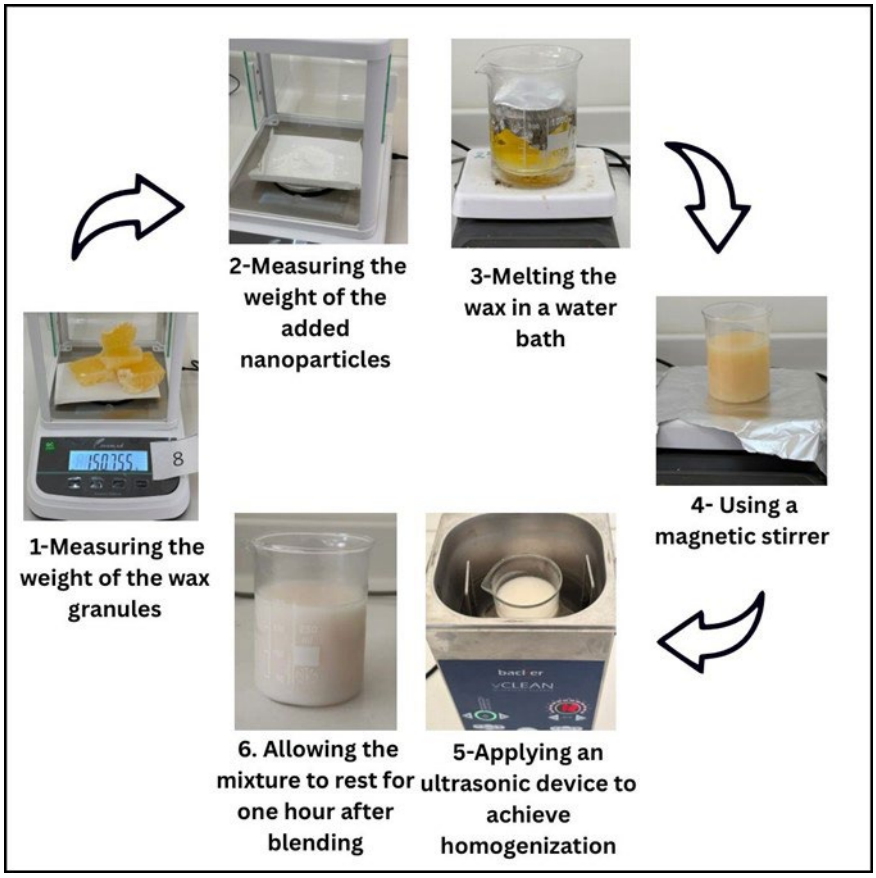

Fig. 2. Steps for mixing paraffin wax with nano magnesium oxide granules

Rys. 2. Etapy mieszania wosku parafinowego z granulkami nanocząsteczkowego tlenku magnezu

2.2. Mechanical stirring method

In this approach, the nanoparticles are directly added to the melted paraffin wax. The mixture is then stirred continuously using a magnetic stirrer for a period ranging between 35 to 50 minutes. The goal is to achieve a fully homogeneous blend, where the nanoparticles are evenly dispersed throughout the wax matrix.

2.3. Ultrasonic dispersion method

For enhanced dispersion, the nanoparticle-wax mixture is placed in an ultrasonic bath. This device emits high-frequency sound waves that create micro-vibrations, helping to break apart any nanoparticle agglomerates and ensuring even suspension within the wax. The ultrasonic treatment is conducted intermittently over the course of one hour at a controlled temperature of 40°C. This temperature is carefully maintained to keep the wax in a liquid state, while avoiding any risk of overheating or degradation. To further prevent the mixture from solidifying during the tube-filling process, a portion of each tube is placed in boiling water to sustain adequate heat. Once the tubes are filled with the nanofluid, the open ends are sealed to prevent any potential leakage, as shown in Figure 3.

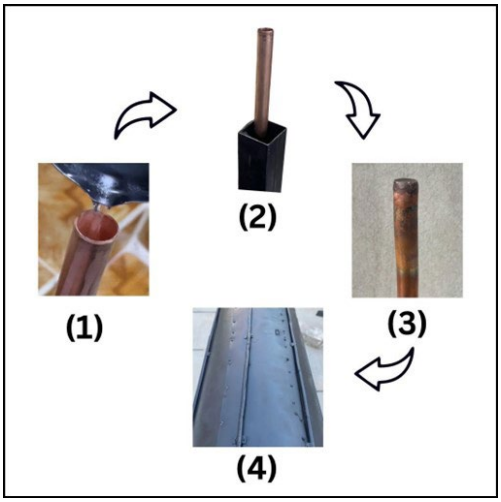

Fig. 3. Steps for filling the wax mixture into the tubes

Rys. 3. Etapy napełniania rurek mieszanką woskową

3. Tools used in the experiment

3.1. The photovoltaic panel

Here are the dimensions of the photovoltaic system that was selected: Its dimensions are L = 1.48 m, W = 0.68 m, and H = 0.035 m. It can handle loads up to 150 W and produces 17.3 Ah of DC power. Its primary role was to supply the charge controller with electricity. The photovoltaic

system was angled at 32 degrees to maximize electrical power generation. The device is made up of four aluminum rods arranged in a rectangle and fastened together with screws at intervals of 0.68 and 1.48 meters. A stationary pedestal is used to set the movable pedestal at different angles. The four supports that attach to the umbrella are made of two pieces of aluminum that are linked at right angles to create a rectangle that matches the measurements of the fixed armrest.

3.2. The controller for solar charging

Using batteries requires the inclusion of an additional critical component known as a solar charge controller. If the batteries are not charged or discharged frequently, their lifespan will be extended. This function is performed by the charge controller. At the point of full battery charging, the charge controller stops the flow of current from the PV modules. Current will be prevented from flowing by the controller until a preset discharge level occurs in the batteries. The majority of charge controllers prohibit the complete discharge of batteries. The extended operational life of the battery depends on the presence of the charger. It is installed behind the solar cell panel.

3.3. The battery

In situations where sunlight is not available, a 70 A heavy-duty calcium battery was used to power the DC motor's driving controller.

3.4. The DC motor controller

A drive-control DC motor adjusted the rotational speed of the hollow cylinder in response to the light intensity. As the sun's rays become more intense, the drive controller raises the hollow cylinder's rotational speed, and when they become less intense, it lowers it. There is a solar intensity sensor built into the drive. As far as sun intensity sensors go, they can be made of photoresistors, light-dependent resistors (LDRs), or photoconductive cells. A photoresistor is a light-controlled variable resistor. By reducing its resistance in response to an increase in the intensity of the incident solar radiation, a photoresistor exhibits photoconductivity. The resistance of the LDR drops significantly when exposed to sunlight, perhaps to a few ohms at the brightest parts of the day. Their resistance can reach 1 M2 when it's dark. LDR devices are considered nonlinear because their sensitivity changes with the wavelength of the light. As

a high-precision integrated circuit, the LDR sensor measures the intensity of the sun's rays. The sensor's output voltage is proportional to the solar intensity. Calibration of the LDR from outside sources is unnecessary. Moreover, it has a 50 KΩ standard variable resistance volume switch that adjusts the circuit's resistance to control the DC motor's power current and voltage. As shown in the electric circuit (6), the charge controller is responsible for supplying power to the drive controlled.

3.5. The DC motor

At the DC motor interface, so that the DC motor can run, the drive controller circuit includes a variable-resistance volume switch. A photovoltaic panel and a charge controller battery are utilized to supply energy to the circuit. A V-belt drives the cylinder-shaped object using the 5.5 Nm torque, 12 V, (0.13–2.59 A), and a DC motor.

a) The measuring instruments:

A TES-1333 type solar power meter, measuring from 0 to 3000 W/m^2, was used to measure the intensity of solar radiation.

b) The temperature measurement:

We used type-K thermocouples to record the temperatures. A digital temperature reading (TES-1310A) and a selector switch were connected to each thermocouple.

c) The graduated cylinder:

In the setup, a graduated cylinder was installed. Units of measurement ranged from 100 to 1000 milliliters, with increments of 10 milliliters. The apparatus was utilized to quantify the overall output of distilled water generated by solar stills. Productivity was recorded using it in conventional and modified solar stills.

d) Air velocity measurement:

Model DA40 digital anemometers were used to measure air velocities. With a precision of 4%, the speed measurement spans from zero to forty meters per second.

Productivity (daily yield per unit area) can be calculated from Equation 1 (Wang et al. 2023):

$$Y = \frac{V_p}{A_t} \tag{1}$$

The productivity, denoted as Y, was expressed in units of either kilograms per square meter per day [kg·m^{-2}·day^{-1}] or milliliters per square meter per day [ml·m^{-2}·day^{-1}]. The collected volume of distilled water was represented by V and measured in cubic meters [m^3] or milliliters [ml]. The density of water, indicated by ρ, was taken as approximately 1,000 kilograms per cubic meter [kg·m^{-3}]. The symbol A referred to the effective collecting area of the solar still in square meters [m^2], while t denoted the measurement period, expressed either in days or seconds.

Energy input from solar irradiance (instantaneous) can be expressed as:

$$Q_{in} = I(t) \cdot A \tag{2}$$

where:

$I(t)$ – solar irradiance [W·m^{-2}],
A – aperture area [m^2].

Evaporative energy can be utilized as follows:

$$Q_{ev} = m_w \cdot h_{fg} \tag{3}$$

where:

m_w – mass of distilled water produced [kg],
h_{fg} – latent heat of vaporization (≈2.26 · 106 J·kg^{-1} at 100°C).

Finally, the thermal efficiency of the still can be calculated from Eq. 4:

$$Efficiency\ \% = \frac{Q_{ev}}{Q_{in}} \tag{4}$$

4. Results and discussion

For three months beginning in February 2025 and ending in April 2025, the system was put through its paces in the Iraqi city of Kirkuk. In order to identify the specific effect on the effectiveness of solar water distillation, numerous experimental studies have been carried out. To put it simply, these are the experiences that have been mentioned. As illustrated in Figure 4, the relationship between freshwater productivity and daylight duration is examined under varying rotational speeds of the hollow cylinder during several days in April 2025 in Kirkuk, Iraq. The results clearly indicate that the total yield of distilled water increases as the rotational speed of the cylinder decreases. This trend can be attributed to the extended exposure to solar radiation during longer daylight hours, which leads to a higher ambient temperature and enhances the evaporation rate of the water layer. The system achieved its highest productivity of 3,300 ml/m^2·day at a rotation speed of 0.25 rpm, whereas a significantly lower output of 1,425 ml/m^2·day was recorded at 3 rpm.

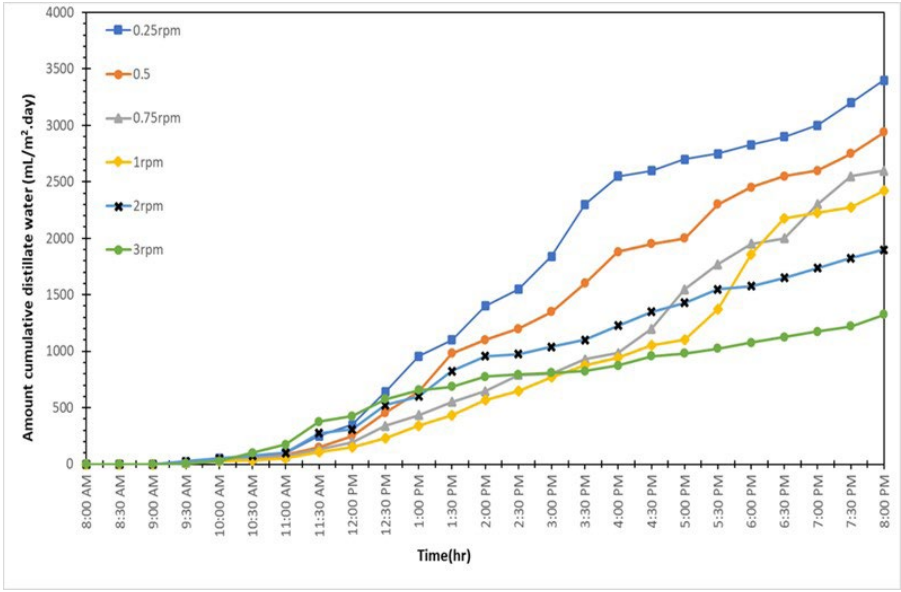

Fig. 4. The effect of cumulative distilled water output as a function of the number of revolutions of the rotating hollow cylinder for different days of April 2025, Kirkuk, Iraq

Rys. 4. Wpływ skumulowanej wydajności wody destylowanej w zależności od liczby obrotów obracającego się cylindra drążonego w poszczególnych dniach kwietnia 2025 r. w Kirkuku w Iraku

Figures 5 and 6 present the distilled water output from both the conventional and the modified solar stills during April 2025. It is observed that the productivity of both systems in April is noticeably higher than that recorded in March and February. This improvement is primarily due to the increased solar radiation intensity during April. Furthermore, the highest yield from the conventional solar still was obtained at a water depth of 3 cm, reaching approximately 520 ml/m^2 · day. In contrast, the modified solar still, which incorporates a PCM enhanced with a composite of paraffin wax and magnesium oxide (PCM + MgO), achieved a significantly higher productivity of around 3,500 ml/m^2 · day.

Figures 7 and 8 show the relationship between daylight hours, ambient temperature, water temperature in the enhanced solar still, and the temperature of the wax mixture with and without MgO nanofluid inside copper tubes for March and April 2025 in Kirkuk, Iraq. The melting process began between 11:00 AM and 12:00 PM and lasted less than 30 minutes due to the thin wax layer. After melting, the mixture continued to absorb heat, with its temperature exceeding that of the basin water by 1:30 PM. Cooling began as solar radiation decreased, with solidification completed around 4:00 PM. The wax mixture with MgO nanofluid maintained higher temperatures than the one without, due to enhanced thermal conductivity. Peak temperatures reached 62°C (with nanofluid) in April, and 46°C (without nanofluid) in March.

Figure 9 illustrates that the wind behavior exhibited noticeable fluctuations depending on the month and the time of day. On February 20, the wind velocity remained relatively low, generally

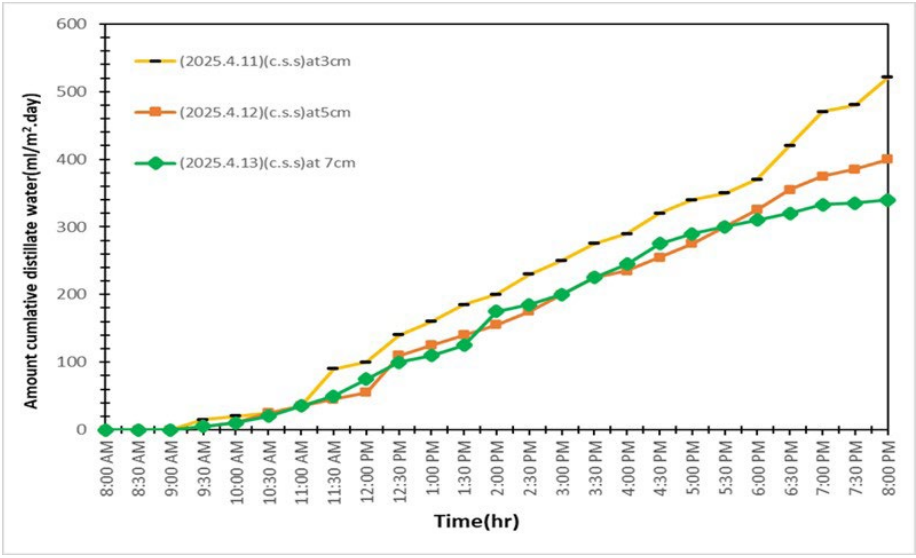

Fig. 5. Relationship between time and productivity with varying basin water depths in a conventional solar still during April 2025 – Kirkuk, Iraq.

Rys. 5. Zależność między czasem a wydajnością przy różnych głębokościach wody w zbiorniku w konwencjonalnej destylarni słonecznej w kwietniu 2025 r. – Kirkuk, Irak.

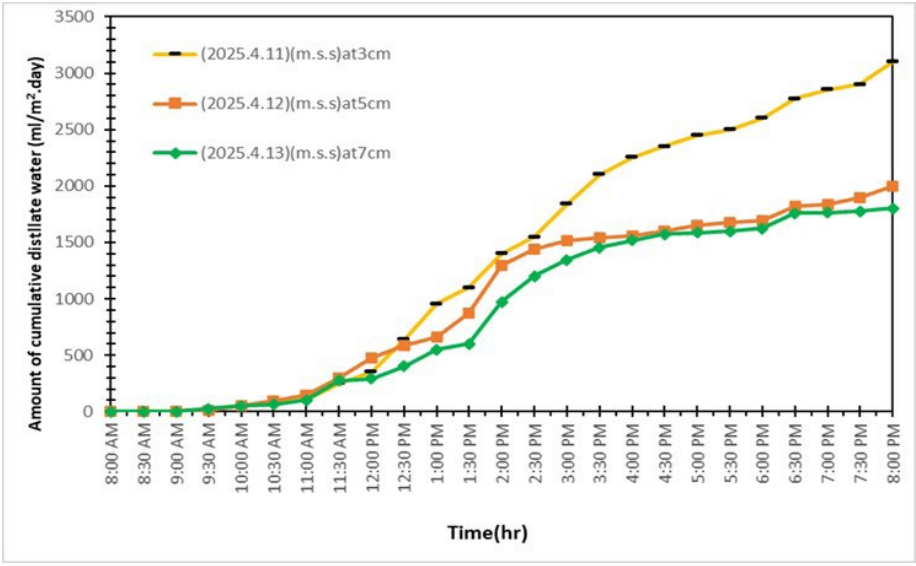

Fig. 6. Relationship between time and productivity with varying basin water depths in the enhanced solar still during April 2025 – Kirkuk, Iraq

Rys. 6. Zależność między czasem a wydajnością przy różnych głębokościach wody w zbiorniku w ulepszonej destylatorze słonecznym w kwietniu 2025 r. – Kirkuk, Irak

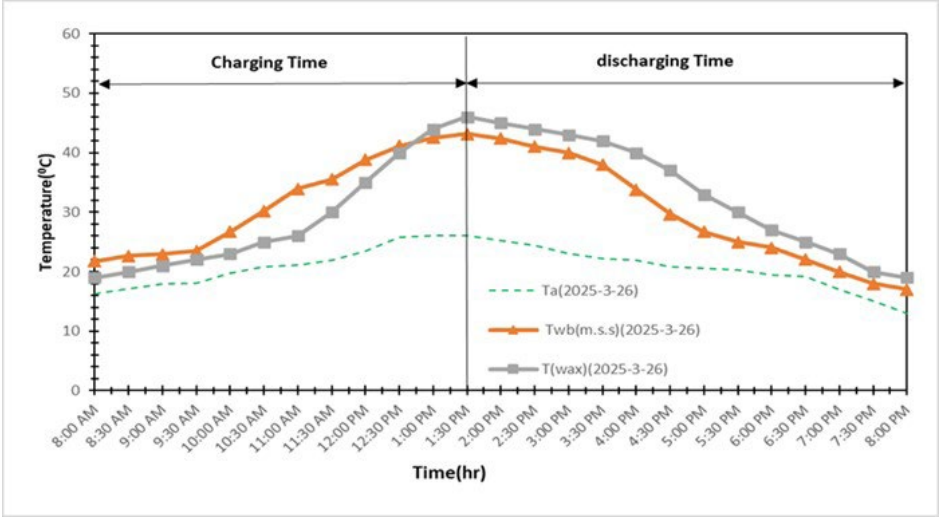

Fig. 7. Relationship between time and temperature of basin water, wax mixture without nanofluid, and ambient air for the enhanced solar distiller (water depth: 3 cm) on March 26, 2025 – Kirkuk, Iraq

Rys. 7. Zależność między czasem a temperaturą wody w zbiorniku, mieszanką woskową bez nanofluidu oraz powietrzem otoczenia dla ulepszonego destylatora słonecznego (głębokość wody: 3 cm) w dniu 26 marca 2025 r. – Kirkuk, Irak

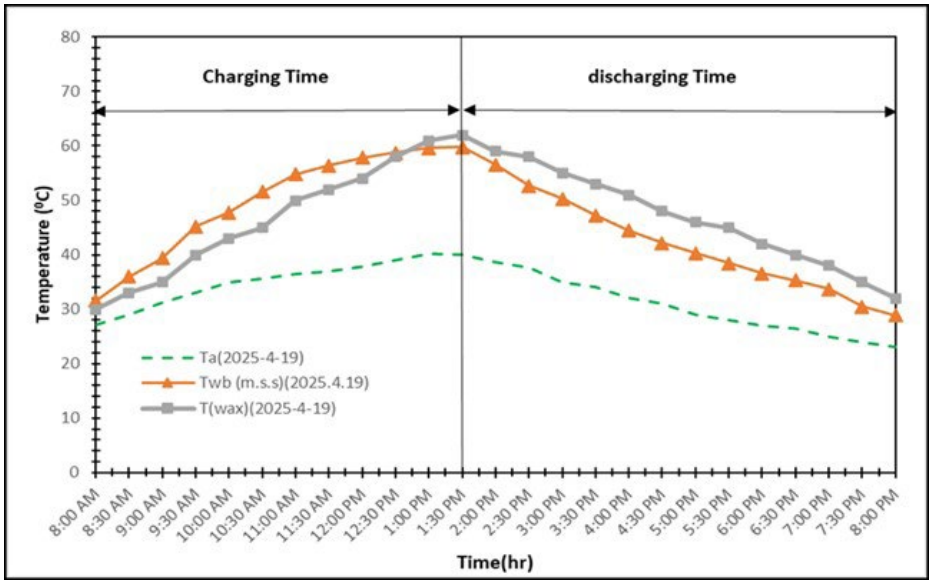

Fig. 8. Relationship between time and temperature of basin water, wax mixture with nanofluid, and ambient air for the enhanced solar distiller (water depth: 3 cm) on April 19, 2025 – Kirkuk, Iraq

Rys. 8. Zależność między czasem a temperaturą wody w zbiorniku, mieszanką woskową z nanofluidem oraz powietrzem otoczenia dla ulepszonego destylatora słonecznego (głębokość wody: 3 cm) w dniu 19 kwietnia 2025 r. – Kirkuk, Irak

below 1.2 m/s, with small peaks observed around 8:00–8:30 AM and 5:30–6:00 PM. In contrast, March 26 recorded the highest wind velocities among the three periods, with values frequently exceeding 2.0 m/s, especially during the morning hours (8:00–10:00 AM) and afternoon periods (2:00–3:30 PM and after 6:30 PM). This indicates that March experienced stronger and more variable winds compared to February and April. Meanwhile, on April 19, the wind velocity was consistently the lowest, staying below 0.5 m/s throughout the day, reflecting very calm atmospheric conditions.

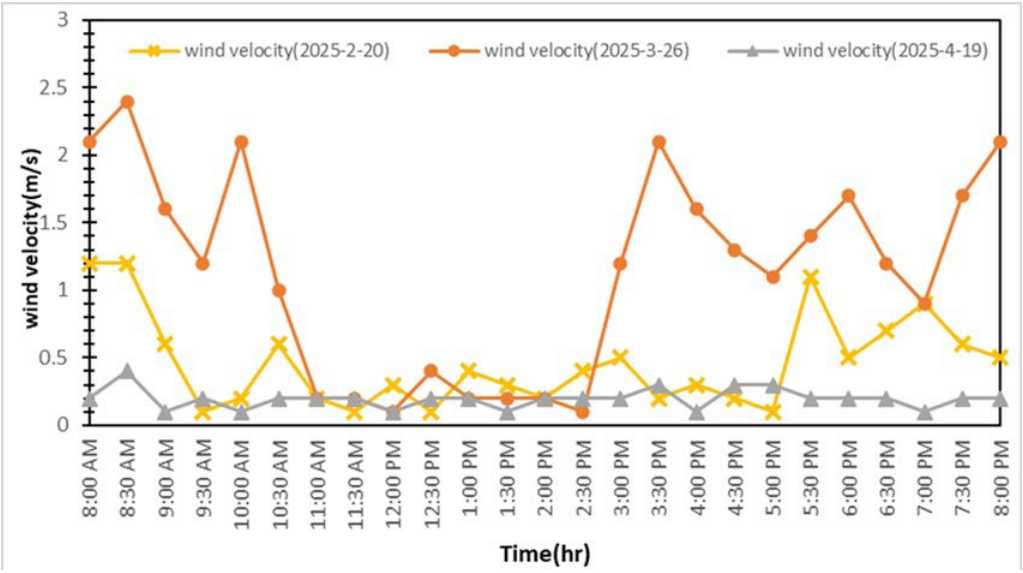

Fig. 9. Relationship between time and wind speed across different months of 2025 – Kirkuk, Iraq

Rys. 9. Zależność między czasem a prędkością wiatru w poszczególnych miesiącach 2025 r. – Kirkuk, Irak

Figure 10 presents a comparison of the productivity of three enhanced solar distillation systems, without additives, with PCM, and with a PCM enhanced by 1% MgO NPCM during day and night across different months in Kirkuk, Iraq (2025). The systems incorporating PCM and NPCM demonstrated continuous water production at night due to their thermal energy storage capabilities, unlike the additive-free system, which functioned only during daylight. The inclusion of MgO nanoparticles in the NPCM improved thermal conductivity, enhancing heat transfer and sustaining higher water temperatures during the melting phase. As a result, the NPCM system achieved the highest productivity: 2,266.67 ml/m$^2 \cdot$ day, compared to 1,533.33 ml/m$^2 \cdot$ day for the PCM system and 1,500 ml/m$^2 \cdot$ day for the system without additives. Notably, the NPCM system also showed superior nighttime performance, indicating its overall efficiency.

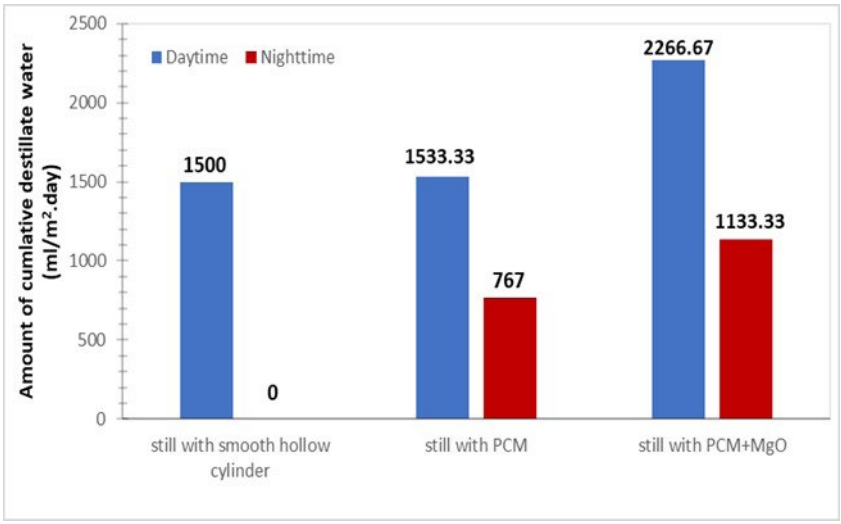

Fig. 10. Daytime and nighttime productivity of various enhanced solar distillation systems across different months – Kirkuk, Iraq (2025)

Rys. 10. Wydajność różnych ulepszonych systemów destylacji słonecznej w ciągu dnia i nocy w poszczególnych miesiącach – Kirkuk, Irak (2025)

Figure 11 illustrates the correlation between daylight duration and the efficiency of a conventional solar still across various months in Kirkuk, Iraq (2025). The conventional system demonstrated the lowest efficiency at 20%, primarily due to its dependence on direct solar radiation without any thermal enhancement. Introducing a smooth hollow cylinder as a heat transfer element raised the efficiency to 52.5%, attributed to the increased heat transfer surface and improved solar absorption. Further improvement was achieved by integrating a PCM, which enabled thermal storage and extended evaporation, resulting in an efficiency of 66.5%. The highest efficiency, 90%, was recorded when using PCM enhanced with MgO nanoparticles, due to improved thermal conductivity, enhanced heat distribution, and faster water heating.

Figure 12 compares the productivity outcomes of the present study with those reported in previous research, focusing on the impact of rotating cylinder surface characteristics on freshwater yield during April 2025 in Kirkuk, Iraq. The highest productivity (~3,400 ml at 0.25 RPM) was obtained using a cylinder surface equipped with copper tubes filled with a paraffin wax-MgO mixture. This configuration enhanced heat transfers due to the increased surface area, leading to higher evaporation rates. In comparison, the perforated aluminum mesh surface produced approximately 2,900 ml, while the smooth surface yielded around 2,050 ml. These findings demonstrate the significant influence of surface modifications on distillation efficiency. However, the productivity in this study remained lower than that reported in (Ali and Ahmed 2024), which utilized a flat-plate water collector with more effective thermal absorption.

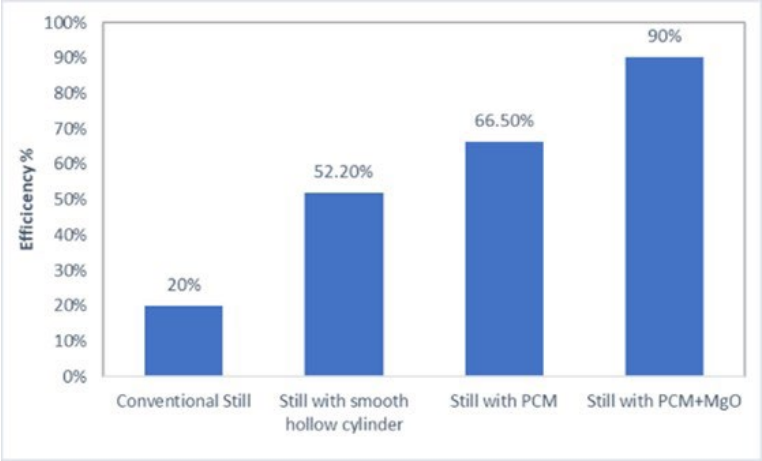

Fig. 11. Efficiency of conventional and enhanced solar stills during different months of 2025 – Kirkuk, Iraq

Rys. 11. Wydajność tradycyjnych i ulepszonych destylatorów słonecznych w poszczególnych miesiącach 2025 r. – Kirkuk, Irak

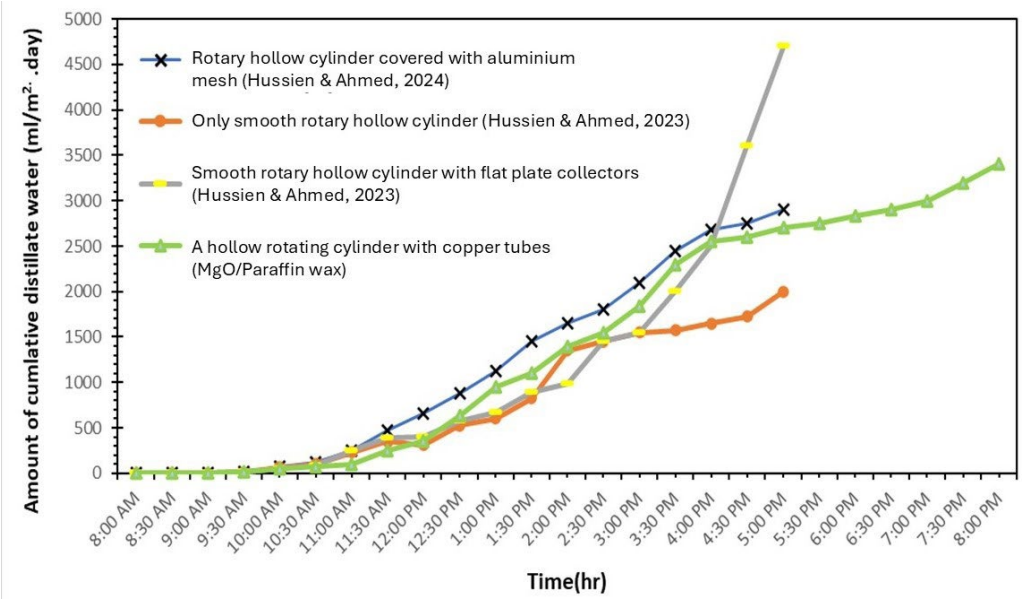

Fig. 12. Comparison of current research productivity with previous studies using different rotating hollow cylinder configurations, smooth surface, smooth surface with flat solar water collector, and aluminum-clamped surface (at 0.25 rpm) in April 2025 – Kirkuk, Iraq

Rys. 12. Porównanie aktualnej wydajności badawczej z wynikami wcześniejszych badań, w których wykorzystano różne konfiguracje obracających się wydrążonych cylindrów: o gładkiej powierzchni, o gładkiej powierzchni z płaskim kolektorem słonecznym oraz o powierzchni z aluminiowymi zaciskami (przy prędkości 0,25 obr./min) w kwietniu 2025 r. – Kirkuk, Irak

Conclusion

The following inferences are drawn from the data collected in this study:

1. It was concluded from this study that the highest productivity for the conventional solar still was obtained at a water depth of 3 cm, reaching 520 ml on April 19. This represented an increase of 25% and 13% compared to depths of 7 cm and 5 cm, respectively. For the enhanced solar still, the highest productivity, 3,400 ml/$m^2 \cdot$ day, was also recorded at a depth of 3 cm, showing an improvement of 14% and 23% when compared to depths of 5 cm and 7 cm, respectively.

2. The maximum temperature of the paraffin wax mixture inside the tubes was recorded in April, reaching 62°C when mixed with nanofluid. In contrast, the temperature of the paraffin wax without the nanofluid reached only 46°C.

3. A maximum productivity of 3,400 ml/$m^2 \cdot$ day was achieved at a rotational speed of 0.25 RPM, while a significantly lower productivity of 1,425 ml/$m^2 \cdot$ day was recorded at 3 RPM.

4. The highest thermal efficiency 90% was achieved using a PCM enhanced with 1% volumetric concentration of MgO nanoparticles. The system using only PCM exhibited an efficiency of approximately 66.5%, while the system with a smooth hollow cylinder reached an efficiency of 52.5%.

The Authors have no conflicts of interest to declare.

References

Abu-Hamdeh et al. 2021 – Abu-Hamdeh, N.H., Alsulami, R.A., Aljinaidi, A.A., Alazwari, M.A., Eltaher, M.A., Almitani, K.H., Alnefaie, K.A., Rawa, M.J.H., Abusorrah, A.M., Sindi, H.F., Salilih, E.M. and Abulkhair, H.A. 2021. Numerical investigation of molten salt/SiO_2 nano-fluid in the solar power plant cycle and examining different arrangements of shell and tube heat exchangers and plate heat exchangers in these cycles. *Journal of the Taiwan Institute of Chemical Engineers* 124, pp. 1–8, https://doi.org/10.1016/j.jtice.2021.05.018.

Alizadeh et al. 2021 – Alizadeh, R., Mesgarpour, M., Ameri, A., Mohebbi Najm Abad, J. and Wongwises, S. 2021. Artificial intelligence prediction of natural convection of heat in an oscillating cavity filled by CuO nanofluid. *Journal of the Taiwan Institute of Chemical Engineers* 124, pp. 75–90, https://doi.org/10.1016/j.jtice.2021.04.067.

Ali, H.H.M. and Ahmed, S.Y. 2023. Exploring the enhancement of solar still performance through the utilization of solar water collectors, rotating hollow cylinders. *International Journal of Machine Tools Maintenance Engineering* 4(1), pp. 9–20.

Ali, H.H.M. and Ahmed, S.Y. 2024. Assessing the economic viability of solar distillation employing a rotating hollow cylinder. *International Journal of Heat and Technology* 42(2), pp. 613–619, https://doi.org/10.18280/ijht.420228.

Ali et al. 2025 – Ali, H.H.M., Danook, S.H. and Mohiuddin, K.O. 2025. Water production from atmospheric air using a solar water recuperator by glass pyramid device. *Tikrit Journal of Engineering Sciences* 32(2), pp. 1–12, https://doi.org/10.25130/tjes.32.2.27.

Ahmed, S.T. and Ali, H.H.M. 2019. Physical and chemical characteristics comparison of the drinking water and water produced from the conventional and modification solar water distillery. *Engineering and Technology Journal* 37(6A), pp. 2014–221, https://doi.org/10.30684/etj.37.6A.5.

Asadpourian, E. and Ameri, A. 2021. Enhancement of solar still productivity using CuO-GO nanocomposite: An experimental approach. *Journal of the Taiwan Institute of Chemical Engineers* 124, pp. 41–52, https://doi.org/10.1016/j.jtice.2021.05.008.

Asbik et al. 2016 – Asbik, M., Ansari, O., Bah, A., Zari, N., Mimet, A. and El-Ghetany, H. 2016. Exergy analysis of solar desalination still combined with heat storage system using phase change material (PCM). *Desalination* 381, pp. 26–37, https://doi.org/10.1016/j.desal.2015.11.031.

Bayraktar et al. 2022 – Bayraktar, N., Abed, F.M. and Ali, H.H.M. 2022. Design, simulation, construction of swimming pools: A comprehensive review. *NeuroQuantology* 20(8), 8922, https://doi.org/10.14704/nq.2022.20.8.NQ44914.

Chaichan, M.T. and Kazem, H.A. 2018. Single slope solar distillator productivity improvement using phase change material and Al_2O_3 nanoparticle. *Solar Energy* 164, pp. 370–381, https://doi.org/10.1016/j.solener.2018.02.049.

Dhindsa, G.S. 2021. Performance enhancement of basin solar still using paraffin wax and floating wicks in the basin. *Materials Today: Proceedings* 37, pp. 3310–3316, https://doi.org/10.1016/j.matpr.2020.09.121.

Fattahi, A. 2021. The effect of cross-section geometry on the performance of a solar nanofluid heater in a parabolic solar receiver: A comparison study. *Journal of the Taiwan Institute of Chemical Engineers* 124, pp. 17–28, https://doi.org/10.1016/j.jtice.2021.05.014.

Hussein et al. 2024 – Hussein, A.M., Ali, H.H.M. and Ali, Z. 2024. Assessing the efficacy of flat-plate solar collectors using nanofluids in the climatic context of Kirkuk city, Iraq. *Acta Polytechnica* 64(1), pp. 25–33, https://doi.org/10.14311/AP.2024.64.0025.

Işık, S.K. and El, E. 2024. Experimental investigation of distilled water production performance of conventional solar stills using $CaCl_2 \cdot 6H_2O$ phase change material reinforced with $SrCl_2 \cdot 6H_2O$ and graphene-based nanoparticles. *Case Studies in Thermal Engineering* 62, https://doi.org/10.1016/j.csite.2024.105184

Kateshia, J. and Lakhera, V. 2022. A comparative study of various fatty acids as phase change material to enhance the freshwater productivity of solar still. *Journal of Energy Storage* 48, https://doi.org/10.1016/j.est.2021.103947.

Kedar et al. 2021 – Kedar, S.A., Bewoor, A.K., Murali, G., Kumar, R., Sadeghzadeh, M. and Issakhov, A. 2021. Effect of reflecting material on CPC to improve the performance of hybrid groundwater solar desalination system. *International Journal of Photoenergy* 2021(1), https://doi.org/10.1155/2021/6675236.

Manoj Kumar et al. 2021 – Manoj Kumar, P., Sudarvizhi, D., Prakash, K.B., Anupradeepa, A.M., Boomiha Raj, S., Shanmathi, S., Sumithra, K. and Surya, S. 2021. Investigating a single slope solar still with a nano-phase change material. *Materials Today: Proceedings* 45, pp. 7922–7925, https://doi.org/10.1016/j.matpr.2020.12.804.

Miri et al. 2023 – Miri, R., Mliki, B., Mohamad, B.A., Abbassi, M.A., Oreijah, M., Guedri, K. and Abderafi, S. 2023. Entropy generation and heat transfer rate for MHD forced convection of nanoliquid in presence of viscous dissipation term. *CFD Letters* 15(12), pp. 77–106, https://doi.org/10.37934/cfdl.15.12.77106.

Motahar et al. 2014 – Motahar, S., Nikkam, N., Alemrajabi, A.A., Khodabandeh, R., Toprak, M.S. and Muhammed, M. 2014. Experimental investigation on thermal and rheological properties of n-octadecane with dispersed TiO_2 nanoparticles. *International Communications in Heat and Mass Transfer* 59, pp. 68–74, https://doi.org/10.1016/j.icheatmasstransfer.2014.10.016.

Nagaraju et al. 2022 – Nagaraju, V., Murali, G., Bewoor, A.K., Kumar, R., Sharifpur, M., El Haj Assad, M. and Awad, M.M. 2022. Experimental study on performance of single slope solar still integrated

with sand troughs. *Sustainable Energy Technologies and Assessments* 50, https://doi.org/10.1016/j.seta.2021.101884.

Qader et al. 2023 – Qader, F., Hussein, A., Danook, S., Mohamad, B. and Khaleel, O. 2023. Enhancement of double-pipe heat exchanger effectiveness by using porous media and TiO_2-water. *CFD Letters* 15(4), pp. 31–42, https://doi.org/10.37934/cfdl.15.4.3142.

Qader et al. 2023 – Qader, F.F., Mohammed, F.Z. and Mohamad, B. 2023. Thermodynamic analysis and optimization of flat plate solar collector using TiO_2/water nanofluid. Journal of Harbin Institute of Technology (New Series), 31(4), pp. 61–73, https://doi.org/10.11916/j.issn.1005-9113.2023050.

Qader et al. 2024 – Qader, F.F., Mohamad, B., Hussein, A.M. and Danook, S.H. 2024. Numerical study of heat transfer in circular pipe filled with porous medium. *Pollack Periodica* 19(1), pp. 137–142, https://doi.org/10.1556/606.2023.00869.

Rufuss et al. 2019 – Rufuss, D.D.W., Rajkumar, V., Suganthi, L. and Iniyan, S. 2019. Studies on latent heat energy storage (LHES) materials for solar desalination application-focus on material properties, prioritization, selection and future research potential. *Solar Energy Materials and Solar Cells* 189, pp. 149–165, https://doi.org/10.1016/j.solmat.2018.09.031.

Rufuss et al. 2022 – Rufuss, D.D.W., Arulvel, S., Kumar, V.A., Davies, P.A., Arunkumar, T. and Sathyamurthy, R. et al. (2022) Combined effects of composite thermal energy storage and magnetic field to enhance productivity in solar desalination. *Renewable Energy* 181, pp. 219–234, https://doi.org/10.1016/j.renene.2021.07.124.

Sharshir et al. 2017 – Sharshir, S.W., Peng, G., Wu, L., Essa, F.A., Kabeel, A.E. and Yang, N. (2017) The effects of flake graphite nanoparticles, phase change material, and film cooling on the solar still performance. *Applied Energy* 191, pp. 358–366, https://doi.org/10.1016/j.apenergy.2017.01.067.

Singh et al. 2023 – Singh, D., Buddhi, D. and Karthick, A. 2023. Productivity enhancement of solar still through heat transfer enhancement techniques in latent heat storage system: a review. *Environmental Science and Pollution Research* 30(1), pp. 44–77, https://doi.org/10.1007/s11356-022-23964-z.

Sonker et al. 2019 – Sonker, V.K., Chakraborty, J.P., Sarkar, A. and Singh, R.K. 2019. Solar distillation using three different phase change materials stored in a copper cylinder. *Energy Reports* 5, pp. 1532–1542, https://doi.org/10.1002/er.5982.

Wang et al. 2023 – Wang, Y., Zhu, Q., Huang, T., Han, X. and Lin, M. 2023. Modelling and simulation of nonlinear dynamic flow field and temperature field of depyrogenation tunnel. *FME Transactions* 51(1), pp. 45–62, https://doi.org/10.22190/FUME221221011W.

Yadav et al. 2021 – Yadav, A., Verma, A., Kumar, A., Dashmana, H., Kumar, A., Bhatnagar, P.K. and Jain, V.K. 2021. Recent advances on enhanced thermal conduction in phase change materials using carbon nanomaterials. *Journal of Energy Storage* 43, https://doi.org/10.1016/j.est.2021.103173.

Yousef, M.S. and Hassan, H. 2019. Energetic and exergetic performance assessment of the inclusion of phase change materials (PCM) in a solar distillation system. *Energy Conversion and Management* 179, pp. 349–361, https://doi.org/10.1016/j.enconman.2018.10.078.

Zarda et al. 2022 – Zarda, F., Hussein, A., Danook, S. and Mohamad, B. 2022. Enhancement of thermal efficiency of nanofluid flows in a flat solar collector using CFD. *Diagnostyka* 23(4), pp. 1–9, https://doi.org/10.29354/diag/156384.

Suzan Abdulrhman Hameed, Hussein Hayder Mohammed Ali, Shahen Mohammed Fakhraldin, Furqan Haider Mohammed Ali

Zwiększanie wydajności termicznej destylatorów słonecznych z wykorzystaniem nanocząsteczek tlenku magnezu w materiale zmieniającym fazę, umieszczonym na obrotowym wydrążonym cylindrze

Streszczenie

W niniejszym badaniu eksperymentalnie zbadano możliwość zwiększenia sprawności cieplnej i wydajności słodkiej wody w destylatorze słonecznym o podwójnym nachyleniu poprzez zastosowanie obrotowego wydrążonego cylindra metalowego w połączeniu z materiałem zmiennofazowym wzbogaconym nanocząstkami (NPCM). Jako nośnik energii cieplnej o cieple utajonym wykorzystano wosk parafinowy, natomiast w celu poprawy przewodności cieplnej i rozkładu ciepła dodano nanocząstki tlenku magnezu (MgO) w stężeniu objętościowym 1%. Nanofluid przygotowano poprzez mieszanie mechaniczne i dyspersję ultradźwiękową w celu zapewnienia jednolitej stabilności. Testy terenowe przeprowadzono w Kirkuku w Iraku w okresie od lutego do kwietnia 2025 r. przy bezchmurnym niebie. Zmodyfikowany system osiągnął maksymalną wydajność około 3400 ml/m^2 · dzień przy 0,25 obr./min i głębokości wody 3 cm, co jest ponad sześciokrotnie wyższą wartością niż 520 ml/m^2 · dzień w przypadku konwencjonalnej destylarni. Włączenie nanocząstek MgO podniosło temperaturę rurki PCM do 62°C w porównaniu z 46°C bez dodatków, zwiększając szybkość parowania i przedłużając produkcję do godzin nocnych. Ulepszona konstrukcja osiągnęła szczytową sprawność cieplną na poziomie 90%, przewyższając systemy oparte wyłącznie na PCM (66,5%) oraz cylindry o gładkiej powierzchni (52,5%). Te korzyści przypisuje się zwiększonej powierzchni wymiany ciepła, lepszej przewodności cieplnej oraz zoptymalizowanej kontroli obrotów. W porównaniu z poprzednimi konstrukcjami cylinder z rurami miedzianymi z NPCM wykazał się lepszą wydajnością. W przyszłych badaniach należy przeanalizować różne rodzaje nanocząstek, możliwość dostosowania do wyższych prędkości obrotowych oraz integrację z hybrydowymi kolektorami słonecznymi, aby jeszcze bardziej zoptymalizować opłacalność i skalowalność rozwiązań w regionach suchych.

Słowa kluczowe: sprawność cieplna, nanocząsteczki tlenku magnezu, materiały zmiennofazowe (PCM), destylator słoneczny, obrotowy wydrążony cylinder